

PROCEEDINGS OF SPIE

SPIDigitalLibrary.org/conference-proceedings-of-spie

Giant pulse generation in the fibers with inscribed Bragg gratings

Aleksei Abramov, Igor Zolotovskii, Vladimir Kamynin, Victor Prikhodko, Aleksei Tregubov, et al.

Aleksei Abramov, Igor Zolotovskii, Vladimir Kamynin, Victor Prikhodko, Aleksei Tregubov, Dmitriy Štol'yarov, Marina Yavtushenko, Andrei Fotiadi, "Giant pulse generation in the fibers with inscribed Bragg gratings," Proc. SPIE 12142, Fiber Lasers and Glass Photonics: Materials through Applications III, 1214212 (25 May 2022); doi: 10.1117/12.2622291

SPIE.

Event: SPIE Photonics Europe, 2022, Strasbourg, France

Giant pulse generation in the fibers with inscribed Bragg gratings

Aleksei Abramov^a, Igor Zolotovskii^{*a}, Vladimir Kamynin^b, Victor Prikhodko^a, Aleksei Tregubov^a,
Dmitry Stoliarov^a, Marina Yavtushenko^a, Andrei Fotiadi^{a,c}

^aUlyanovsk State University, 42 Leo Tolstoy Street, Ulyanovsk 432970, Russia; ^b Prokhorov
General Physics Institute of the Russian Academy of Sciences, 38 Vavilov st., Moscow, 119991,
Russia; ^cElectromagnetism and Telecommunication Department, University of Mons, Mons, B-
7000, Belgium

ABSTRACT

In this paper it was investigated the dynamics of frequency-modulated pulses in fiber cascades, consisting of a fibers with sequentially formed refractive index gratings with different periods. It is shown that the proposed scheme can be used to generate picosecond and subpicosecond pulses with peak powers of the order of ~ 1 MW. In the considered cascade structures, it is shown that it is possible to form stable sequences of pico- and subpicosecond pulses with a subterahertz repetition rate directly from continuous wave signals as a result of a modulation instability regime.

Keywords: generation of ultrashort pulses; fiber Bragg gratings; frequency modulated pulse temporal compression; modulation instability.

1. INTRODUCTION

The fiber laser technology has recently been raised with the emerging ultrashort pulse (USP) sources emitting the pulses of high peak power. Such laser sources are of great demand for a variety of applications, e.g., material processing, cut edging, precise surface structuring, surgical procedures. In science and metrology, USP lasers are used with ultrafast spectroscopy, multiphoton microscopy or optical coherence tomography [1,2]. An achievement of higher pulse peak power in fiber lasers is associated with the use of optical fibers possessing a low nonlinearity [3]. Among such fiber materials are single-mode fibers with large mode area ($>100 \mu\text{m}^2$) [4-6], step- or grade-index tapered fibers [5,7,8]. Besides, the optical fibers with the dispersion varying along the fiber length are commonly used for the generation of high peak power USP [1-3]. Such fibers enable as well pulse compression, supercontinuum generation, and optical processing [9,10]. Therefore, design of nonuniform fibers possessing low nonlinearity is of great practical interest for high-power USP fiber lasers. However, precise control of the fiber dispersion parameters is a technically challenging task. In particular, in grade-index (parabolic) and step-index tapered fibers, the group velocity dispersion (GVD) is determined by the fiber material dispersion and could not be tailored. A simple way to overcome this limitation is to inscribe the array of refractive index fiber Bragg gratings with different periods distributed along the fiber length in a proper way. This concept has been demonstrated to control the frequency-modulated (FM) pulse dynamics in Ref. [11–13].

Currently, the FBG fabrication is a well-established technique [14], in particular, it is widely used with grade-index multimode fibers promising for applications in high energy and high peak power laser pulsed sources [15–17]. In this paper, we describe the method enabling amplification and temporal compression of FM pulses in a fiber configuration comprising both passive and active (amplifying) fibers with the inscribed refractive index fiber Bragg gratings (FBGs) of different periods. We demonstrate that in combination with the tapered fiber such a fiber configuration could be used for generation of ultrashort pulse train with a high repetition rate (terahertz) directly from the input weakly modulated CW light.

2. FIBERS WITH INSCRIBED FBG ARRAYS

Let us consider the dynamics of an optical signal propagating in a fiber with the inscribed FBG arrays (Figure 1). The refractive index variation along FBG is defined by the function [9-12]:

$$n_i(z) = n_0 \left[1 - m \cos(2\pi z / \Lambda_i(z)) \right], \quad (1)$$

where n_0 is the fiber average refractive index, m is the modulation depth of the inscribed grating, Λ_i is the period of the i -th FBG, $i = 1, 2, \dots$. Contribution of the refractive index changes in FBG to the (GVD) is known to dominate the fiber material dispersion. The second-order GVD is expressed as [9,10]:

$$\beta_2(z) = d_2 - \frac{\text{sign}(\delta) \cdot \kappa^2}{V_g^2 (\delta^2 - \kappa^2)^{3/2}} = \frac{1}{c} \left(\frac{\partial^2 (\omega n_0(\omega))}{\partial \omega^2} \right)_{\omega=\omega_0} - \frac{\text{sign}(\delta) \cdot \kappa^2}{V_g^2 (\delta^2 - \kappa^2)^{3/2}}, \quad (2)$$

where d_2 is the fiber material second-order dispersion, V_g is the group velocity of the pulse propagating in the fiber without FBGs, $\kappa = 2\pi m / \lambda_0$ is the coefficient describing the coupling between the forward and backward waves, λ_0 is the central optical signal wavelength, δ_i is the normalized detuning of the optical signal carrier frequency from the peak FBG reflectivity frequency ω_B . For a uniform FBG, this detuning can be written as [15,16,18]:

$$\delta_i(z) = \frac{\omega_0 - \omega_{Bi}(z)}{V_g} = \frac{2\pi c}{V_g} \left(\frac{1}{\lambda_0} - \frac{1}{\lambda_{Bi}(z)} \right) = \frac{2\pi c}{V_g \lambda_0} - \frac{\pi}{\Lambda_i(z)}. \quad (3)$$

Depending on $\Lambda_i(z)$ the detuning $\delta_i(z)$ can be either negative or positive. Correspondingly, the second-order GVD of the fiber is normal or anomalous at $\delta < 0$ and $\delta > 0$, respectively. Here in after, the pulse wavelength is assumed to be less than and far from the FBG peak reflectivity wavelength, i.e. $\delta \gg \kappa$. In this case, Eq. (2) is reduced to:

$$\beta_2(z) = d_2 - \frac{\kappa^2}{V_g^2 \delta^3}, \quad (4)$$

The FBG reflectivity spectrum bandwidth is $\Delta\lambda_{gap} = m\lambda_0 / 2n_0 \ll 1$ nm. At a large frequency detuning $\delta \gg \kappa$, the inscribed FBG has no effect on the effective cubic nonlinear coefficient in the fiber, since it is determined by the fiber material only. However, the contributions of higher-order dispersion coefficients still have to be taken into account. In particular, the third-order GVD contribution is expressed as [10,18]:

$$\beta_3(z) = d_3 + \frac{3\delta\kappa^2}{V_g^3 (\delta^2 - \kappa^2)^{5/2}} = \frac{1}{c} \left(\frac{\partial^3 (\omega n_0(\omega))}{\partial \omega^3} \right)_{\omega=\omega_0} + \frac{3\kappa^2}{V_g^3 \delta^4}, \quad (5)$$

In accordance with Eq. (5), the parameter $\beta_3(z)$ in a single-mode fiber is several orders of magnitude higher than the material third-order dispersion d_3 [9,10] and so it can deteriorate the FM pulse compression quality resulting in pulse shape distortion and even decay.

Let the period $\Lambda_i(z)$ of FBGs inscribed in the optical fiber increase along the fiber length z . In this case, δ also increases with z leading to the decrease of the anomalous GVD absolute value. As follows from Eqs.2 and 5, the second- and third-order dispersion parameters decrease as δ^{-3} and δ^{-4} , respectively. The contributions of higher-order dispersion ($\beta_n \sim \delta^{-n}$) reduce even faster, thereby preventing the shape deformation for the generation of high peak power subpicosecond pulses considered below.

3. SOLITON-LIKE FM PULSE TEMPORAL COMPRESSION IN FIBERS WITH INSCRIBED FBG

The dynamics of pulse propagation in an optical fiber with the inscribed FBG arrays (Figure 1) could be described by the nonlinear Schrödinger equation commonly used with nonuniform fibers [19,20] and taking into account the fiber nonlinearity, gain factor, second- and third-order dispersion coefficients:

$$\frac{\partial A}{\partial z} - i \frac{\beta_2(z)}{2} \frac{\partial^2 A}{\partial \tau^2} - \frac{\beta_3(z)}{6} \frac{\partial^3 A}{\partial \tau^3} + iR(z) \left(|A|^2 - \tau_R \frac{\partial |A|^2}{\partial \tau} \right) A = g(z)A, \quad (6)$$

where $\tau = t - \int_0^z d\xi / u(\xi)$ is the time in the running reference frame, $u(z)$ is the pulse group velocity, $\beta_{2,3}(z)$ are the second- and third-order dispersion parameters, $R(z)$ is the cubic (Kerr) nonlinearity coefficient, $g(z)$ is the gain factor, τ_R is the nonlinear (Raman) response time in the fiber medium. At $\beta_3(z) \rightarrow 0$ and $\tau_R \rightarrow 0$, the pulse evolution described by Eq. (6) could exhibit unlimited temporal compression resulted in unlimited increase of the peak amplitude [19]. To get this solution, the dispersion and nonlinear coefficient should be kept unchangeable along the fiber with anomalous GVD ($\beta_2 R < 0$) and the gain factor distribution determined by the function $g(z) = g_0 / (1 - 2g_0 z)$ should be provided. In this case, in the fiber length $2g_0 z < 1$, the pulse evolution described by Eq. (6) is expressed as:

$$A(\tau, z) = \frac{A_0}{1 - 2g_0 z} \operatorname{sech} \left(\frac{\tau}{\tau_s} \right) \exp \left(i \frac{\alpha_0 \tau^2 - \Gamma z}{1 - 2g_0 z} \right). \quad (7)$$

Here, A_0, τ_s, α_0 are the input pulse amplitude, duration, and FM rate, respectively, $\Gamma = g_0 / 2\alpha_0 \tau_0^2$. Similar scenario of the FM soliton pulse evolution is also achievable in the optical fiber with a constant gain but the GVD varying along the fiber length. To get this operation in the active fiber with a constant gain factor, the GVD profile has to be described as [21,22]:

$$\beta_2(z) \rightarrow -|\beta_{20}| \exp \left[-\frac{\alpha_0 |\beta_{20}|}{g_0} (\exp(2g_0 z) - 1) + 2g_0 z \right]. \quad (8)$$

It results in evolution of the pulse duration:

$$\tau(z) \rightarrow \tau_0 \exp \left[-\frac{\alpha_0 |\beta_{20}|}{g_0} (\exp(2g_0 z) - 1) \right]. \quad (9)$$

For passive fibers with $g_0 = 0$, Eqs. (8, 9) are reduced to:

$$\beta_2(z) \approx -|\beta_{20}| \exp(-2\alpha_0 |\beta_{20}| z), \quad (10)$$

$$\tau_s(z) \approx \tau_0 \exp(-2\alpha_0 |\beta_{20}| z). \quad (11)$$

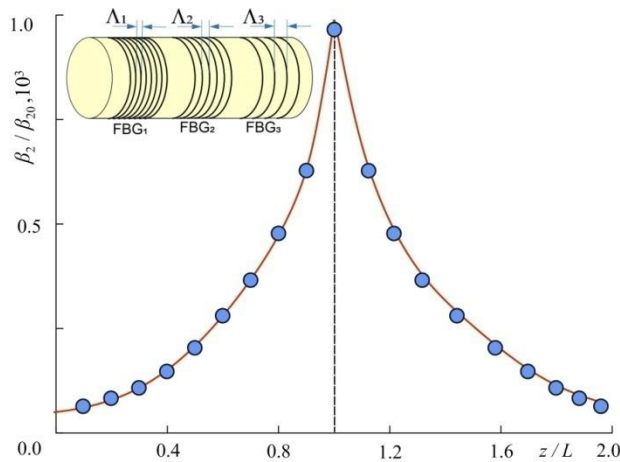


Figure 1. Arrangement of the second-order dispersion profile in the cascaded fiber configuration comprising one active and one passive fiber. The length of active and passive fiber segment is $l = 22.5$ cm, $g_1 = 0.2$ cm⁻¹ and $g_2 = 0$. On inset is optical fiber segment comprising three FBGs with increasing period.

Therefore, under the condition that the proper GVD profile is provided by a proper distribution of the inscribed FBG period along the fiber length, the fibers with the inscribed FBG arrays could be employed for the generation of high peak power USPs.

Let us consider the dynamics of FM pulse propagating in a passive or active optical fiber with the inscribed FBG array (Figure 1). All inscribed FBGs differ only in the period Λ_i , where i is the FBG order number. The average refractive index $n_0 = 1.5$ and modulation depth m are assumed to be the same for all FBGs. In the numerical calculations, we use the parameters typical for standard optical fibers and inscribed gratings: the cubic nonlinearity coefficient $R = 10^{-3} (\text{W} \cdot \text{m})^{-1}$ at the wavelength $\lambda_0 = 1550 \text{ nm}$, mode effective area $S_{\text{eff}} = 50 \mu\text{m}^2$ nonlinear response time of medium $\tau_R \approx 5 \cdot 10^{-15} \text{ s}$, $d_2 = -2 \cdot 10^{-27} \text{ s}^2/\text{m}$, $d_3 = 10^{-40} \text{ s}^3/\text{m}$ [10]. It is worth noting that the parameter d_2 can play a crucial role at the final stage of pulse compression, when the light bandwidth is maximal and the effect of the inscribed FBG on the dispersion is minimal. The used parameters of the inscribed FBGs are the Bragg wavelength $\lambda_{\text{B1}}(z=0) \equiv 2n_0\Lambda_1 = 1556.5 \text{ nm}$, detuning $\delta \approx 2.5 \cdot 10^4 \text{ m}^{-1}$, and refractive index modulation depth $m = 5 \cdot 10^{-4}$. The coupling coefficient $\kappa \approx 2.5 \cdot 10^3 \text{ m}^{-1}$ corresponds to these parameters. The proper distribution of the FBG period along the fiber length is used to provide the exponential GVD profile $\beta_2(z) = -|\beta_{20}| \exp(-qz)$.

4. AMPLIFICATION AND TEMPORAL COMPRESSION OF FM PULSES IN A CASCADE OF FIBERS

Amplification and temporal compression of pulses will be consider in the cascaded configuration comprising active and passive fibers of the same length L with the inscribed FBGs. A gradual decrease of the FBG period down to a certain minimal value corresponds to the GVD increase.

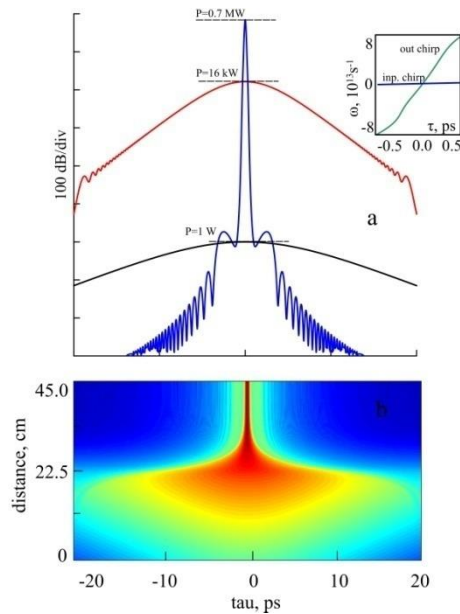


Figure 2. Temporal compression of FM pulse in the cascaded fiber configuration comprising one active and one passive fibers. The parameters: duration $\tau_0 = 10 \text{ ps}$, initial power $P_0 = 1 \text{ W}$, initial frequency modulation $\alpha_0 = 10^{24} \text{ s}^{-2}$, nonlinearity $R = 10^{-5} (\text{W} \cdot \text{m})^{-1}$ and dispersion profile are shown in Figure 1.

In the cascaded fiber configuration, the first fiber has a constant uniform gain $g_1 > 0$ along the whole fiber length, whereas in the second passive fiber $g_2 = 0$. In the first fiber, the inscribed FBG period smoothly decreases, whereas in

the second segment it smoothly increases getting the initial level. The period of each FBG is set so that the GVD profile shall be approximated by the exponential functions $\beta_2 = \beta_{20} \exp(\pm qz)$ (Figure 3). In the first fiber, the FBG period decreases from 517.5 to 529.2 nm and the GVD increases by the factor $\beta_2 / \beta_{20} \approx 10^3$. In the second fiber, the GVD decreases exponentially down to its original value β_{20} .

Figure 2 shows the shape (a) and evolution (b) of the pulse as it propagates in the fiber cascade. In the active fiber, the input pulse experiences rather weak pulse temporal compression and its power (black curve) increases up to $P \approx 16$ kW (Figure 2, red curve). In the passive fiber, a strong temporal compression with a drastic increase of the peak power up to a megawatt level occurs (Figure 2, blue curve). Importantly, the pulse FM at the cascade output is nearly linear (Figure 2, inset). So, the pulse is suitable for further temporal compression by standard tools, like a pair of diffraction gratings.

CONCLUSION

We have explored evolution of the FM pulses in the fiber cascaded configurations comprising one active and one passive optical fibers with the inscribed FBG arrays. Both amplification and temporal compression in such a fiber cascade resulting in peak powers up to ~ 700 kW are theoretically described. The quality of generated pulse increases with the number of FBGs inscribed in the fiber of the given length. We have shown that the amplified pulses could possess the linear frequency chirp making them available for further compression.

REFERENCES

- [1] Geddes, C.G., Toth, C., Tilborg, J., Esarey, E., Schroeder, C.B., Bruhwiler, D., Nieter, C., Cary, J., and Leemans, W.P., "High-quality electron beams from a laser wakefield accelerator using plasma-channel guiding," *Nature* 431, 538 (2004).
- [2] Buck, A., Wenz, J., Karsch, S., and Veisz, L., "Shock-front injector for high-quality laser-plasma acceleration," *Phys. Rev. Lett.* 110, 185006 (2013).
- [3] Renninger, W.H., and Wise, F.W., "Optical solitons in graded-index multimode fibres," *Nat. Commun.* 4, 1719 (2013).
- [4] Krupa, K., Tonello, A., Shalaby, B.M., Fabert, M., Barthélémy, A., Millot, G., Wabnitz, S., and Couderc, V., "Spatial beam self-cleaning in multimode fibres," *Nat. Photonics* 11, 237 (2017).
- [5] Agrawal, G. P., "Imaging in multimode graded-index fibers and its impact on the nonlinear phenomena," *Opt. Fiber Technol.* 50, 309-316 (2019).
- [6] Filippov, V., Chamorovskii, Yu., Kerttula, J., Golant, K., Pessa, M., and Okhotnikov, O.G., "Double clad tapered fiber for high power applications," *Opt. Express* 16, 1929-1944 (2008).
- [7] Trikshev, A.I., Kurkov, A.S., Tsvetkov, V.B., Filatova, S.A., Kerttula, J., Filippov, V., Chamorovskiy, Yu.K., and Okhotnikov, O.G., "A 160 W single-frequency laser based on an active tapered double-clad fiber amplifier," *Laser Phys. Lett.* 10, 065101 (2013).
- [8] Andrianov, A. V., Koptev, M. Yu., Anashkina, E. A., Muravyev, S. V., Kim, A. V., Lipatov, D. S., Velmiskin, V. V., Levchenko, A. E., Bubnov, M. M., and Likhachev, M.E., "Tapered erbium-doped fibre laser system delivering 10 MW of peak power," *Quantum Electron.* 49, 1093 (2019).
- [9] Kivshar, Yu.S., and Agrawal, G.P., "Optical Solitons: From Fibers to Photonic Crystals," Academic Press: New York, USA, 125 (2003).
- [10] Agrawal, G.P., "Nonlinear fiber optics," 4th ed.; Springer: New York, USA, 530 (2007).
- [11] Litchinitser, N.M., Eggleton, B.J., and Patterson, D.B., "Fiber Bragg gratings for dispersion compensation in transmission: theoretical model and design criteria for nearly ideal pulse recompression," *J. of Lightwave Tech.* 15, 1303-1313 (1997).
- [12] Lenz, G., and Eggleton, B.J., "Adiabatic Bragg soliton compression in nonuniform grating structures," *JOSA B: Opt. Phys.* 15, 2979-2985 (1998).

- [13] Qui, L., Wai, P.K.A., Senthilnathan, K., and Nakkeeran, K., "Modeling self-similar optical pulse compression in nonlinear fiber Bragg grating using coupled mode equation," *J. of Lightwave Tech.* 29, 1293-1305 (2011).
- [14] Kablukov, S.I., Zlobin, E.A., Skvortsov, M.I., Nemov, I.N., Wolf, A.A., Dostovalov, A.V., and Babin, S.A., "Mode selection in a directly diode-pumped Raman fibre laser using FBGs in a graded-index multimode fibre," *Quantum Electron.* 46, 1106 (2016).
- [15] Zlobina, E.A., Kablukov, S.I., Wolf, A.A., Dostovalov, A.V., and Babin, S.A., "Nearly single-mode Raman lasing at 954 nm in a graded-index fiber directly pumped by a multimode laser diode," *Opt. Lett.* 42, 9 (2017).
- [16] Wolf, A., Dostovalov, A., Bronnikov, K., and Babin, S., "Arrays of fiber Bragg gratings selectively inscribed in different cores of 7-core spun optical fiber by IR femtosecond laser pulses," *Opt. Express* 27, 13978 (2019).
- [17] Sang, X., Yu, C., and Yan, B., "Bragg gratings in multimode optical fibers and their applications," *J. of Opt. and Adv. Mat.* 8, 1616 (2006).
- [18] Kashyap, R., "Fiber Bragg gratings," Academic Press (1999).
- [19] Sang, X., Yu, Ch., and Yan, B., "Bragg gratings in multimode optical fibres and their applications," *J. of Optoelect. and Adv. Mat.*, 8, 1616-1621 (2006).
- [20] Jha, R., Villatoro, J., and Badenes, G., "Ultraprecise in reflection photonic crystal fiber modal interferometer for accurate refractive index sensing," *Appl. Phys. Lett.* 93, 191106 (2008).
- [21] Korobko, D. A., Okhotnikov, O. G., and Zolotovskii, I. O., "High-repetition-rate pulse generation and compression in dispersion decreasing fibers," *JOSA B.* 2377-2386 (2013).
- [22] Korobko, D. A., Okhotnikov, O. G., Stoliarov, D. A., Sysoliatin, A. A., and Zolotovskii, I. O., "Highly nonlinear dispersion increasing fiber for femtosecond pulse generation," *J. of Lightwave Tech.* 33, 3643-3648 (2015).